# Study on Weight-Optimized Shielding Design for Micro-Reactor Deployment in Korea

Jin Sun Choi, Jeong Ik Lee

Dept. Nuclear & Quantum Eng., KAIST, 373-1, Guseong-dong, Yuseong-gu, Daejeon, 305-701, Republic of Korea \*Corresponding author: jeongiklee@kaist.ac.kr

#### 1. Introduction

The potential for domestic deployment of micro hightemperature gas-cooled reactors (HTGRs) has attracted attention in diverse applications, including distributed power supply and industrial process heat utilization.

Although HTGRs employing TRISO fuel are characterized by inherent safety and simplified system configurations, the compact core scale results in significant increases in neutron leakage and gamma emission. These characteristics present an engineering challenge in which both shielding performance and mass must be simultaneously considered.

Historically, the ASTR (1955, U.S. airborne reactor used to study crew shielding for a nuclear-powered aircraft) incorporated approximately 15.9 tons of shielding, which imposed constraints on airborne payload capacity, whereas the ML-1 (1962, U.S. trailer-mounted mobile nuclear power plant for remote Army sites) exceeded highway axle load limits due to the additional shielding mass [1-2].

More recently, lightweight shielding concepts have been investigated, such as composite shielding developed by CPS Technologies and the Nuclear Grade Sandwich Composite (NGSC) design studied at INL based on the Pele Project [3-4].

However, only limited quantitative studies have evaluated shielding performance under design constraints relevant to domestic deployment, including ISO transport standards and site space limitations.

In this study, a 10 MW $_{th}$  HTGR referenced to the PBMR-400 was analyzed using MCNP to compare the attenuation performance of candidate shielding materials, and multilayer configurations were evaluated to assess the potential for weight reduction.

### 2. Methodology

In this study, HTGRs were primarily considered as the most suitable microreactor type for domestic deployment. By employing TRISO fuel, HTGRs are provided with high fuel integrity and strong radionuclide retention capability, thereby ensuring safety [5].

In addition, due to the multilayer coated-particle

structure and the inherent difficulty of reprocessing, advantages are conferred in terms of nuclear nonproliferation and security. The ability to supply a high-temperature heat source of 750–950°C makes HTGRs suitable for meeting domestic demands for industrial process heat and hydrogen production.

Furthermore, their scalability and modularity, as well as the application of passive safety systems, provide benefits under domestic regulatory and siting constraints. Based on these characteristics, the HTGR was selected as the reference reactor type for this study, as it was considered consistent with national industrial demands and operating conditions.

### 2.1 Reference Model and Assumptions

As the reference model, the PBMR-400 HTGR reactor design was used due to the data availability. The reference reactor was linearly scaled down to a thermal power of 10 MWth and adopted as the steady-state analysis model. At the reflector boundary, the neutron flux was estimated to be  $1.58 \times 10^{13}$  n/cm<sup>2</sup>·s and the gamma flux  $1.52 \times 10^{12}$  y/cm<sup>2</sup>·s for the 10MW<sub>th</sub> reactor.

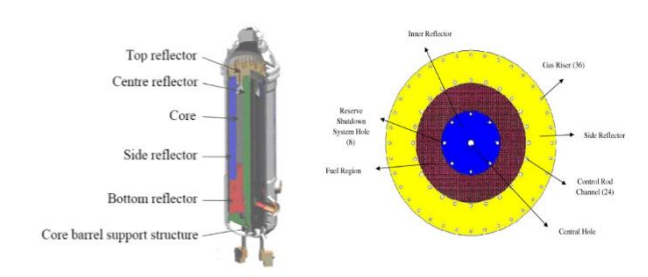


Fig 1. PBMR-400 design [6].

Table 1. PBMR-400 Characteristics [6].

PBMR Characteristic	Value
Installed thermal capacity	$400 { m MW_{th}}  (165 { m MW_e})$
Fuel	TRISO ceramic coated U-235
Primary coolant	Helium
Reflector	Graphite
Core temperature	900 / 500 °C (outlet / inlet)

Transport and installation constraints were applied following the INL Pele Project specifications, with a shielding thickness limited to 40 cm and a total mass restricted to 76.1 tons [4].

# 2.2 Candidate Shielding Materials

Based on a literature review, four candidate shielding materials—including hydrides, borides, and high-density metals—were selected, as summarized in Table 2. In the selection process, attenuation performance for both neutron and gamma flux after a thickness of 5 cm was evaluated.

Table 2. Flux after 5cm thick of shield [7-10].

Neutron—gamma	1		
performed using MCI	NP 6.2. A V	Watt fission	spectrum,
approximating the ch	aracteristics	of core leal	kage, was
applied as the source	term, and t	he number o	of particle
histories was set to	$NPS=1\times10^{\circ}$	to ensure	statistical
convergence of relativ	e errors.		

2.3 MCNP Analysis and Verification

	Material	Neutron flux after 5cm thick shield (n/cm²·s)	Gamma flux after 5cm thick of shield (γ/cm²·s)	Density (g/cm³)	Neutron attenuation	Gamma attenuation	Temperature stability
	Water (H <sub>2</sub> O)	$9.42 \times 10^{12}$	1.09 × 10 <sup>12</sup>	0.997	0	$\nabla$	abla
Existing	HD-Polyethylene (PE)	$8.78 \times 10^{12}$	$1.14 \times 10^{12}$	0.95	0	$\nabla$	$\nabla$
	Lead (Pb)	$1.34 \times 10^{13}$	$2.87 \times 10^{10}$	11.35	$\nabla$	0	$\nabla$
	Concrete	$1.33 \times 10^{13}$	$7.07 \times 10^{11}$	2.4	$\nabla$	Δ	$\nabla$
	$ZrH_2$	$7.54 \times 10^{12}$	$2.88 \times 10^{11}$	5.6	0	0	$\circ$
Advanced	$TiH_2$	$6.22 \times 10^{12}$	$5.43 \times 10^{11}$	3.75	0	Δ	$\circ$
	$\mathrm{B_{4}C}$	$6.27 \times 10^{12}$	$7.70 \times 10^{11}$	2.52	0	Δ	$\circ$
	$TiB_2$	$6.63 \times 10^{12}$	$3.92 \times 10^{11}$	4.52	0	0	$\circ$
	$ZrB_2$	$6.61 \times 10^{12}$	$2.45 \times 10^{11}$	6.10	0	0	0
	W	$1.11 \times 10^{13}$	$8.39 \times 10^{9}$	19.25	Δ	0	0
	$W_2B_5$	$5.22 \times 10^{12}$	$1.69 \times 10^{10}$	15.25	0	0	0
	WC	$1.12 \times 10^{13}$	$1.25 \times 10^{10}$	14.3	Δ	0	0
	W-Ni-Fe	$1.12 \times 10^{13}$	$1.02 \times 10^{10}$	17.2	Δ	0	©
* Effectiv	reness Note: ▽(Very Low)	△ (Moderate)	○ (Good) ◎ (Very hig	gh)			

Additionally, criteria were applied to ensure thermal and chemical stability at elevated temperatures consistent with steady-state HTGR operating conditions.

The selected materials were further classified according to their dominant shielding function: hydride-based materials were applied on the inner side to provide thermal and epithermal neutron attenuation through elastic scattering, while high-density metallic materials were arranged on the outer side to enhance gamma-ray and fast neutron attenuation. The multilayer configuration was constructed with the total thickness of 40 cm, equally divided into 20 cm for the inner and outer layers, as shown in Fig. 2

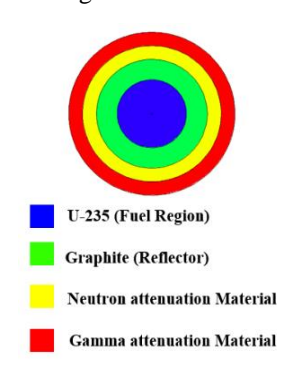


Fig 2. Schematic of HTGR Core and Multilayer Shielding Model

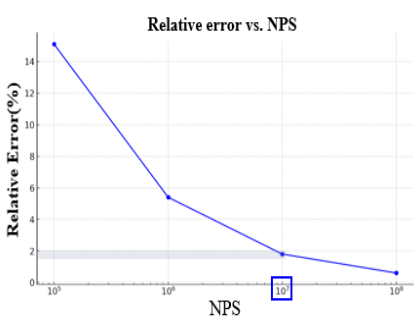


Fig 3. NPS Reliability Verification: Relative Error

The leakage flux deviation in the homogenized TRISO-fuel model was within  $\pm 3\%$ , indicating that reliable results could be obtained even with the simplified model.

Table 3. Neutron Leakage: Homogeneous vs. Heterogeneity TRISO [6].

	Homogeneous	Heterogeneity	Relative error
Total Neutron leakage	37.2%	38.4%	+3.2%
Leakage out of system	0.191	0.197	+3.1%

### 3. Results

As a result, hydrides exhibited strong performance in thermal and epithermal neutron attenuation, whereas borides were found to be effective for thermal neutron absorption.

## 3.1 Energy-Dependent Performance

Figure 4 presents the attenuation ratios of candidate shielding materials across neutron spectral energy ranges.

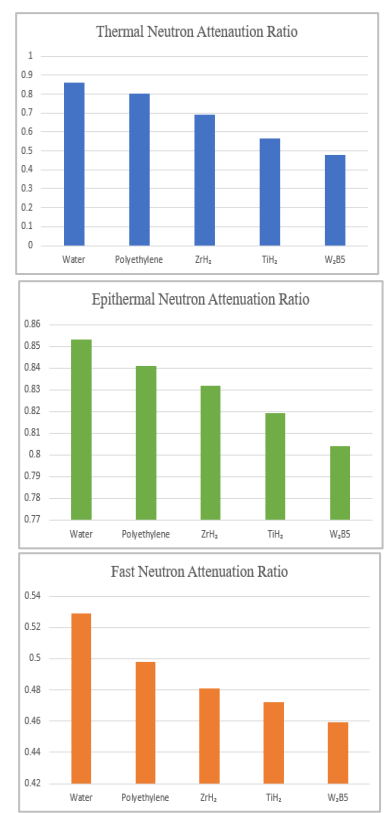


Fig 4. Attenuation Ratio by Energy Range for Different Shielding Materials

Since the graphite reflector had already moderated and absorbed a substantial portion of thermal neutrons, the differences in attenuation ratios among materials in the thermal region were relatively small.

In contrast, distinct variations were observed in the epithermal and fast regions due to differences in material-specific cross sections and interaction mechanisms.

In particular,  $W_2B_5$  exhibited stable and superior attenuation performance over the entire spectrum, attributed to the combined effects of the  $^{10}B$  (n,  $\alpha$ ) reaction and inelastic scattering by tungsten.

# 3.2 Multilayer Shielding Design

The multilayer design was configured by separating the primary shielding functions: hydride-based neutron shielding materials were placed on the inner side, and high-density metallic gamma shielding materials were placed on the outer side.

Table 4 summarizes the shielding performance of four candidate multilayer combinations evaluated under the fixed 40 cm thickness constraint. With respect to the 76.1 t mass limit, the hydride–ZrB $_2$  configurations (ZrH $_2$ +ZrB $_2$  and TiH $_2$ +ZrB $_2$ ) satisfied the requirement, whereas the W $_2$ B $_3$ -based combinations exceeded the constraint.

Table 4. Shielding Performance of Candidate Material Combinations

	Total Mass (t)	N-attenuation ratio	γ-attenuation ratio
Water + Pb	85.4	$3.88 \times 10^{2}$	5 × 10 <sup>4</sup>
ZrH2 +	75.4	$6.74 \times 10^{3}$	$7.41 \times 10^{5}$
ZrB2	75.4	0.74 ^ 10	7.41 ^ 10
ZrH2 +	140.6	$3.64 \times 10^{4}$	$3.23 \times 10^{6}$
$W_2B_5$	140.0	3.04 × 10	3.23 × 10
TiH <sub>2</sub> +	63.6	$8.68 \times 10^{3}$	8.74 × 10 <sup>5</sup>
ZrB2	03.0	6.06 ^ 10	6.74 ^ 10
TiH <sub>2</sub> +	128.1	$4.66 \times 10^{4}$	$3.99 \times 10^{6}$
$W_2B_5$	126.1	4.00 ^ 10	3.99 ^ 10

- \* Neutron flux:  $1.58 \times 10^{13}$  / Gamma flux:  $1.52 \times 10^{12}$
- \* Attenuation Ratio =  $\phi_{in} / \phi_{out}$
- \* Total mass includes end-caps; layer thickness fixed at 20 cm (inner) + 20 cm (outer)

As shown in Fig. 5, the hydride–ZrB<sub>2</sub> design achieves both low mass and high attenuation, while W<sub>2</sub>B<sub>5</sub>-based stacks shift toward the high-mass, high-performance region, illustrating the inherent trade-off between shielding effectiveness and structural weight.

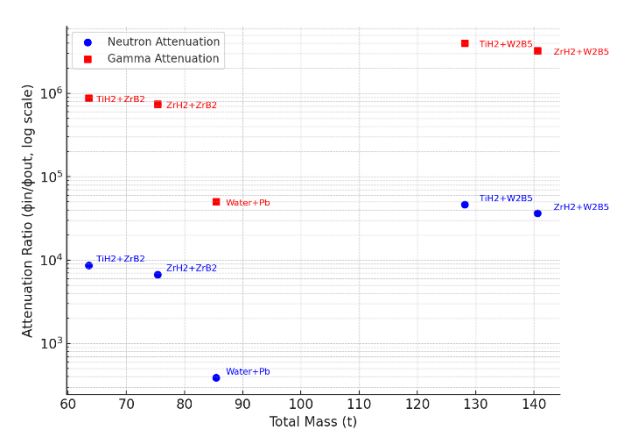


Fig 5. Shielding mass–attenuation trade-off of candidate multilayer combinations

Compared with the conventional water—lead reference, the hydride—ZrB<sub>2</sub> configurations achieved up to 25% less total mass (63.6 t vs. 85.4 t), highlighting their advantage in lightweight shielding. Hydrides primarily attenuate thermal and epithermal neutrons, while the outer high-density layer enhances fast-neutron and gamma shielding.

In contrast, the  $W_2B_5$ -based designs, despite delivering  $\sim 1-2$  orders of magnitude higher  $\gamma$ -attenuation than the reference, resulted in substantially higher total mass

(128–141 t), indicating limited benefits for weight reduction under the fixed 20 cm+20 cm layer configuration.

This points to the need for thickness-ratio optimization (e.g., a thinner  $W_2B_5$  layer) to balance dose reduction and structural mass.

### 4. Conclusion

In this study, MCNP analyses were conducted on a 10 MWth HTGR model referenced to the PBMR-400 to evaluate the potential for weight reduction in shielding design for domestic deployment. Candidate shielding materials, including hydrides, borides, and high-density metals, were assessed, and the results confirmed that multilayer configurations provide engineering advantages over single-material designs in terms of both shielding performance and weight efficiency.

In particular, the combination of hydrides and  $W_2B_5$  demonstrated superior neutron–gamma composite shielding effectiveness but did not meet the 76.1 t mass limit under the current 20 cm + 20 cm configuration; further optimization of thickness ratios or adoption of graded-Z arrangements will be required to reconcile attenuation effectiveness with mass efficiency.

These findings highlight a promising alternative for shielding design under the high neutron leakage conditions of micro-HTGRs. Future application should incorporate optimized thickness ratios and dose-based evaluations to achieve both shielding performance and weight efficiency.

In addition, worker dose assessments aligned with domestic regulatory standards are essential to verify feasibility for weight-optimized shielding in Korea's microreactor deployment.

# **ACKNOWLEDGEMENTS**

This work was supported by the National Research Foundation of Korea (NRF) grant funded by the Korea government (MSIT) (No.: RS-2024-00436693).

#### REFERENCES

- [1] Pacific Northwest National Laboratory, Microreactor transportability challenges (2021).
- [2] Pacific Northwest National Laboratory, Microreactor transportation emergency planning challenges (2024).
- [3] CPS Technologies, Radiation shielding and metal matrix composites (2024).
- [4] Idaho National Laboratory, Preliminary analysis of Nuclear Grade Sandwich Composite for transportable micro reactor shielding (2024).
- [5] Kim, SongYee, Feasibility Study on Deploying Microreactors in the Republic of Korea (ROK) Army (2025)
- [6] IAEA, Evaluation of High Temperature Gas Cooled Reactor Performance: Benchmark Analysis Related to the PBMR-400, PBMM, GT-MHR, HTR-10 and the ASTRA Critical Facility (2013)
- [7] Carpenter D, Thermal and Irradiation Performance of Zirconium Hydride Moderators (2023)
- [8] Cinbiz M.N. et al., Considerations for Hydride Moderator Readiness in Micro-reactors (2023)
- [9] Lin Y.R, Response of <sup>11</sup>B-Enriched ZrB<sub>2</sub> Ultra-High-Temperature Ceramic to Neutron Irradiation (2024)
- [10] S.E. Bays, Shielding of Transportable Fission Batteries: Issues and Potential Solutions, INL/MIS-22-69958 (2022)